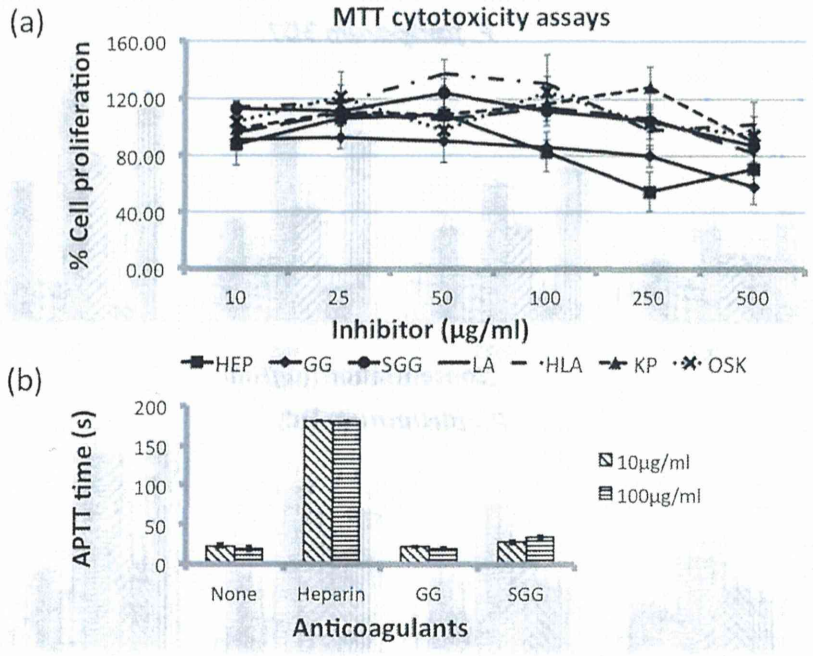

Figure 3 | Cytotoxicity and Activated Partial Thromboplastin Time (APTT) assays (a) Cytotoxicity assays using 293T cells. Cultures of 293T cells (100 μl) were seeded into 96-well flat-bottom plates and incubated at 37°C. At about 50% confluence, the old media were replaced with fresh media containing the inhibitors heparin (HEP), gellan gum (GG), gellan sulfate (SGG), λ-carrageenan (LA), hydrolyzed λ-carrageenan (HLA), κ-carrageenan (KP), or oversulfated κ-carrageenan (OSK) and the cells were incubated at 37°C for 48 h. MTT (10 μl) was then added to the cultures, which were kept in the dark overnight (about 12 h) at room temperature. Absorbance was read at 595 nm and the % cell viability was computed as: % cell viability = (absorbance$_{595\ nm}$ of treated group ÷ absorbance$_{595\ nm}$ of control group) × 100%. Means and standard deviations from the means were computed from triplicates assays in three independent experiments. (b) APTT assays. Pooled plasma from adult C57BL/6 and BALB/c mice were used for the APTT anticoagulant assays. 10 μl of heparin, gellan gum, and gellan sulfate each diluted in PBS were mixed with 100 μl of plasma for final concentrations of 10 and 100 μg/ml and then incubated at 37°C for 1 minute. The APTT assays were performed using Drihemato® APTT Test Reagent Card (A&T Corporation, Japan) according to manufacturer's instructions. Coagulation times (in seconds) were read in a Drihemato® system Coag2V machine. Two independent experiments for each assay were performed in triplicates and means and standard deviations were calculated.

gellan sulfate were 28.7 s and 35.7 s, respectively (Figure 3B). For plasma with native gellan gum, mean APTT times were 22.5 s at 10 μg/ml, and 19.7 s at 100 μg/ml. These data demonstrate that our synthesized gellan sulfate does not have strong anticoagulant activity.

Discussion

Polysaccharides from marine sources are currently gaining popularity for their potential medical and therapeutic applications. Seaweed-derived polysaccharides such as carrageenans[23] and fucoidan[50] have been shown to inhibit the growth and invasion of *P. falciparum in vitro*. However, in *in vivo* studies, although a decrease in parasitemia may have been observed, there was no significant improvement in the recovery of mice from the illness[24,50]. In addition, λ-carrageenan was found to increase the permeability of the blood-brain barrier of rats when injected subcutaneously[25], which could aggravate the disease by adding to the development of cerebral malaria.

Although the exact mechanism of inhibition by these sulfated polysaccharides has yet to be defined, it appears to involve the interactions of the malarial invasion proteins with the sulfated proteoglycans, like heparan sulfate and chondroitin sulfate, that are present on the surface of most cell types including erythrocytes. These interactions have been demonstrated by Boyle *et al.*[18] and our group[17,19], which showed that heparin interacts with the invasion proteins MSP1 and EBA-140.

Naturally occurring polysaccharides have been modified by sulfation and assessed for their anticoagulant, antibacterial, and antiviral activities. Galactomannans from seed extracts were modified by sulfation and shown to have activities against yellow fever virus and dengue 1 virus *in vitro* and *in vivo*[51], and against HIV *in vitro*[52]. Sulfated konjac glucomannans have also been shown to act against HIV[53].

Modification of κ-carrageenan improves its action against a variety of pathogens. Low molecular weight κ-carrageenan (3 kDa) and κ-carrageenan oligosaccharides (KOS), as well as their sulfated derivatives have anti-influenza virus effects both *in vitro* and *in vivo*[30,31]. KOS had also enhanced immunostimulatory and antitumor activities[26,27]. In addition, κ-carrageenan that was covalently bound to 3′-azido-3′-deoxythymidine AZT, was found to be active against HIV *in vitro*[32].

Gellan sulfate has been prepared for use in various medical applications, for example, as an artificial ligand to remove the extra domain A containing fibronectin (EDA(+)FN) from the plasma of rheumatoid arthritis patients[42], and as a novel anticoagulant[43].

For these reasons, we synthesized oversulfated κ-carrageenan and gellan sulfate to assess their activities against malaria parasites *in vitro*. Elemental analysis showed that our synthesized oversulfated κ-carrageenan and gellan sulfate had sulfate contents of 13.6% and 9.57%, respectively (Table 1). The degree of substitution values (DS) were calculated as 3.0 for κ-carrageenan and 3.7 for gellan[54,55]. Note that the maximum DSs for carrageenan and gellan are 4.0 and 10.0, respectively. Thus, sulfation rates (%) of κ-carrageenan and gellan sulfate relative to their maximum DSs were calculated as 75% and 37%.

The synthesized oversulfated κ-carrageenan and hydrolyzed λ-carrageenan showed no activity against *Plasmodium* parasites, which differs from the findings of previously reported studies with modified carrageenans. These differences could be attributed to the different

modes of invasion and replication of the viruses within host cells compared with that of parasites.

Our results show that our synthesized gellan sulfate effectively inhibited both the growth and invasion of the *P. falciparum* merozoites *in vitro* unlike the native gellan gum yet similar to heparin. However, unlike heparin, gellan sulfate is a potential artificial ligand for EDA(+)FN from the plasma of rheumatoid arthritis patients because it does not bind to proteins such as plasma fibronectin and antithrombin III[42]. Yet, gellan sulfates with 17.5% sulfation or greater were found to be potent anticoagulants, like heparin in APTT assays by Miyamoto *et al.*[43]. In our cytotoxicity and anticoagulant assays, our synthesized gellan gum, with 37% sulfation was found to have low cytotoxicity and anticoagulant activity. However, at present, we cannot determine the exact reason for these different results. Given that there is insufficient information about the effects of gellan sulfate *in vivo*, and considering these results, it is suggested that the synthesized gellan sulfate must be used with caution in future *in vivo* studies. It will also be of interest to explore the mechanism by which gellan sulfate inhibits growth and invasion of red blood cells by the *Plasmodium* parasite. In future studies, we intend to investigate if gellan sulfate can inhibit parasite adhesion to the red blood cell similar to other glycosaminoglycans, and how the gellan sulfate molecule interacts with the *Plasmodium* parasite invasion proteins that interact with heparin such as MSP1 and BAEBL.

Methods

Polysaccharides and sulfation of κ-carrageenan and gellan gum. The polysaccharides used in this study were heparin and λ-carrageenan (Sigma-Aldrich, St. Louis, Mo.), and κ-carrageenan and gellan gum (WAKO Pure Chemical Ltd. Co., Osaka, Japan). Hydrolyzed λ-carrageenan, oversulfated κ- carrageenan, and gellan sulfate were synthesized as Yuan *et al.*[26] with modifications.

λ-carrageenan (1% (w/v) in distilled water) was hydrolyzed with 0.1 M HCl to pH 4.0 for 1 h at 70°C[26] with stirring. The reaction was neutralized with $NaHCO_3$ and filtered. The supernatant was concentrated by evaporation and desalted by dialysis against distilled water for 48 h at 4°C using a Cell Sep H1 tube (MWCO 1,000, Orange Scientific Inc. Belgium). The retained solution was lyophilized and dried *in vacuo* for 24 h at room temperature.

κ-carrageenan was sulfated by an SO_3-pyridine complex, as previously described[26]. Two grams of lyophilized κ-carrageenan (from a 1% (w/v) solution in distilled water) was added to *N,N*-dimethylformamide (DMF) (84 ml) at 60°C for 30 min. To this mixture, 16 ml of SO_3-DMF complex was added and the mixture was stirred for 4 h at 70°C. The SO_3-DMF complex was prepared by dropping 20 ml of $ClSO_3H$ into 100 ml of DMF in an ice water bath. After cooling to room temperature, the mixture was neutralized with saturated $NaHCO_3$ solution, dialyzed against deionized water for 2 days, and the dialysate was freeze-dried to give sulfated κ-carrageenan. Gellan (1% (w/v)) was treated with 0.1 M HCl up to pH 3.0. The acid-treated gellan gum (insoluble fraction) was recovered by filtration and extensively washed until neutralized and then lyophilized. Sulfation was carried out in the same manner as for κ-carrageenan to give gellan sulfate. The degree of substitution (DS) of the sulfonyl group for κ-carrageenan and gellan was defined as the molar number of sulfonyl group per di-saccharide and tetra-saccharide units. DS was calculated based on elemental analysis, according to the equation given by Rochas *et al.*[54] as follows: DS = (S%/*atomic mass of S*)/(C%/*atomic mass of C* × *number of carbons for one unit*). Atomic masses of C and S are 12 and 32, respectively. The numbers of carbons in one unit of carrageenan and gellan are 12 and 24, respectively. The sulfation rate (%) was calculated by taking the ratio of the DS of the sulfonyl group to the maximum DS of 4 for κ-carrageenan and 10 for gellan.

Prior to being added to the cultures, the polysaccharides were dissolved in distilled water to a concentration of 2 mg/ml, and then filtered through a 0.22-μm filter and further diluted with appropriate complete media. Polysaccharides that were insoluble at room temperature, namely κ-carrageenan, λ-carrageenan, and gellan gum, were dissolved in distilled water at 80°C; heparin, oversulfated κ-carrageenan, hydrolyzed λ-carrageenan, and gellan sulfate were dissolved at room temperature.

Analytical methods. ^{13}C NMR spectra were obtained from a JEOL 500 MHz spectrometer operating at 500 MHz. The spectra for the oversulfated κ-carrageenan were recorded at 25°C, whereas the spectra for the native gellan gum and the gellan sulfate were recorded at 90°C. Chemical shifts (δ in ppm) were expressed relative to the resonance of D_2O (^1H NMR) ($\delta = 4.8$) and DMSO (^{13}C NMR) ($\delta = 39.5$). Samples for NMR analysis were dissolved in DMSO (oversulfated κ-carrageenan = 60 mg/ml; native gellan gum = 5 mg/ml; gellan sulfate = 20 mg/ml) and trace amounts of D_2O were subsequently added.

The concentration of S was analyzed with an Ion Chromatography System Dionex ICS-1100/1600 (Thermo Scientific Inc., MA USA). The concentration of C was analyzed with a 2400 Series II CHNS/O System (Perkin Elmer Inc., MA, USA). DS was calculated using the formula of Rochas *et al.*[54] as described earlier.

***In vitro* culture of *Plasmodium falciparum* parasites.** The chloroquine-sensitive line *Plasmodium falciparum* 3D7 and the chloroquine-resistant line, *P. falciparum* Dd2 parasites were maintained in continuous culture as described by Radfar *et al.*[56]. In this method, the parasites are grown in human A^+ red blood cells and maintained in culture medium containing RPMI 1640, 25 mM HEPES, 100 μM hypoxanthine, 12.5 μg/ml gentamicin sulfate supplemented with 2.5% (w/v) Albumax II, and 62.5 μg/ml of $NaHCO_3$. Cultures were kept at 37°C, 5% CO_2, and 5% O_2, with daily medium changes; conditions were maintained at 1% hematocrit and 1% parasitemia.

Cell culture. Human embryonic kidney derived 293T cells were grown at 37°C, 5% CO_2, and 5% O_2 in culture medium containing DMEM, L-glutamine, penicillin-streptomycin, and 62.5 μg/ml $NaHCO_3$, supplemented with 10% fetal calf serum and passaged every two days at 70%–80% confluency.

Growth inhibition. Growth inhibition assays (GIAs) were performed as previously described[57]. Predominantly ring stage cultures were first synchronized by sorbitol treatment. GIAs were carried out at the next day, when the cultures were mostly in the late trophozoite stage. Infected red blood cells were mixed with fresh Type A^+ RBCs to make cultures with 0.30% parasitemia and 1% hematocrit. A 25-μl aliquot of culture was then transferred into 96-well plates and 2.5 μl of the inhibitors was added to each well such that the final concentrations were 9, 4.5, 2.25, and 0.9 μg/ml. Three independent experiments were performed and all were done in triplicate; parallel cultures were also maintained. The cultures were incubated at 37°C, with 5% CO_2, and 5% O_2. At 48 h post-incubation, 5 μl of complete medium was added to each culture. Flow cytometry was used to determine the parasitemia after 90–96 h when the parasites were mostly in the trophozoite-schizont stages.

Flow cytometry. Flow cytometry was used to determine the parasitemia of the cultures[57]. Cultures were mixed with 10 μg/ml ethidium bromide in PBS and left at room temperature for 1 h in the dark. The cell pellets were then resuspended in 500 μl of PBS and transferred into flow cytometry tubes. Flow cytometric analysis was carried out on a FACSCalibur cell analyzer (BD Biosciences) and the data were analyzed with WinMDi ver. 2.9.

Invasion inhibition. For the invasion inhibition assays[58,59], cultures were purified by using a MACS® (Miltenyl Biotec, Japan) magnetic bead separation column to obtain trophozoite and schizont stage parasites. Purified schizonts were mixed with complete medium to obtain hematocrit of 1%, and fresh A^+ red blood cells were added for a total parasitemia of 5% with ring stage parasitemia of almost 0%. Cultures (100 μl) were transferred into 96-well plates and the inhibitors heparin, gellan gum, and gellan sulfate were added to a final concentration of 10 μg/ml. Cultures were incubated for 20 h at 37°C, with 5% CO_2 and 5% O_2. For this, two independent assays were done in duplicates.

Assessment of invasion inhibition. Culture supernatants were aspirated and the cell pellets were smeared and stained with Giemsa staining to determine ring stage parasitemia. Means and standard deviations of ring stage parasitemia were obtained, and the percent inhibition was computed by using the following formula: [Eq.2] {(Mean% Ring stage parasitemia of untreated cultures – Mean% Ring stage parasitemia of inhibitor-treated cultures) ÷ Mean% Ring stage parasitemia of untreated cultures} × 100%.

Cytotoxicity assays. MTT assays were performed using 293T cells. Cells were seeded in 96-well flat-bottom plate with a culture volume of 100 μl at a 2 : 1000 dilution and incubated at 37°C, 5% CO_2, and 5% O_2. After 24 h, at about 50% confluency, the old media were aspirated and replaced with 100 μl of complete medium containing inhibitors at concentrations of 500, 250, 100, 50, 25, and 10 μg/ml. The cells and inhibitors were then incubated at 37°C, 5% CO_2, and 5% O_2 for 48 h. MTT solution (10 μl of 5 mg/ml) was added to the culture, which was kept in the dark at room temperature overnight. The following morning, the old media were aspirated and 100 μl of DMSO was added as an MTT solvent. The cells were then assessed by measuring absorbance at 595 nm and the % cell viability was computed as follows[60]: [Eq. 3] % cell viability = ($absorbance_{595\ nm}$ of treated group ÷ $absorbance_{595\ nm}$ of control group) × 100%.

***In vitro* anticoagulant activated partial thromboplastin time (APTT) assay.** APTT assays were carried out using plasma from healthy mice[49]. Blood was collected from the hearts of normal adult female C57BL/6 and BALB/c mice under terminal anesthesia. The blood was immediately mixed with 3.2% trisodium citrate at a 9 : 1 blood: anticoagulant ratio. Plasma was obtained by spinning the blood in a bench top centrifuge for 15 minutes and was then pooled. Heparin, gellan gum, and gellan sulfate (10 μl) each diluted in PBS were mixed with 100 μl of plasma for a final concentration of 10 and 100 μg/ml and then incubated at 37°C for 1 minute. The APTT assays were performed using the Drihemato® APTT Test Reagent Card (A&T Corporation, Japan) according to manufacturer's instructions. Coagulation times were recorded in seconds (s).

Animals. Adult female C57BL/6 and BALB/c mice purchased from CLEA Japan (Tokyo, Japan) were maintained in controlled light and dark conditions and given food and water ad libitum.

Ethical statement. The protocol for animal use in experiments was approved by the Committee on the Animal Experiments of the Obihiro University of Agriculture and Veterinary Medicine (Permission No. 25-153, 2013). Animal experiments were conducted in accordance with the Guidelines for Animal Experimentation of the Japanese Association for Laboratory Animal Science and the Fundamental Guidelines for Proper Conduct of Animal Experiment and Related Activities in Academic Research Institutions under the jurisdiction of the Ministry of Education, Culture, Sports, Science and Technology, Japan.

1. World Health Organization. *World malaria report: 2012.* http://www.who.int/malaria/publications/world_malaria_report_2012/wmr2012_full_report.pdf (2012). Date accessed: March 27, 2014.
2. Kweka, E. J. *et al.* Challenges to malaria control and success stories in Africa. *Glob. Health Perspect.* **1**, 71–80 (2013).
3. Sherman, I. W. *Malaria: Parasite Biology, Pathogenesis and Protection.* (ASM Press, 1998).
4. Yahata, K., Treeck, M., Culleton, R., Gilberger, T. W. & Kaneko, O. Time-lapse imaging of red blood cell invasion by the rodent malaria parasite *Plasmodium yoelii. PLoS One* **7**, e50780. (2012).
5. Schwartz, L., Brown, G. V., Genton, B. & Moorthy, V. S. A review of malaria vaccine clinical projects based on the WHO rainbow table. *Malar. J.* **11**, (2012).
6. Cowman, A., Berry, D. & Baum, J. The cellular and molecular basis for malaria parasite invasion of the human red blood cell. *J. Cell Biol* **198**, 961–971 (2012).
7. Gaur, D. & Chitnis, C. E. Molecular interactions and signaling mechanisms during erythrocyte invasion by malaria parasites. *Curr. Opin. Microbiol.* **14**, 422–428 (2011).
8. Harvey, K. L., Gilson, P. R. & Crabb, B. S. A model for the progression of receptor-ligand interactions during erythrocyte invasion by *Plasmodium falciparum. Int. J. Parasitol.* **42**, 567–573 (2012).
9. Kulane, A. *et al.* Effect of different fractions of heparin on *Plasmodium falciparum* merozoite invasion of red blood cells *in vitro. Am. J. Trop. Med. Hyg.* **46**, 589–594 (1992).
10. Clark, D. L., Su, S. & Davidson, E. A. Saccharide anions as inhibitors of the malaria parasite. *Glycoconjugate J.* **14**, 473–79 (1997).
11. Xiao, L.,Yang, C., Patterson, P. S., Udhayakumar, V. & Lal, A. A. Sulfated polyanions inhibit invasion of erythrocytes by *Plasmodium* merozoites and cytoadherence of endothelial cells to parasitized erythrocytes. *Infect. Immun.* **64**, 1373–1378 (1996).
12. Bastos, M. F. *et al.* Fucosylated chondroitin sulfate inhibits *Plasmodium falciparum* cytoadhesion and merozoite invasion. (abstract) *Antimicrob Agents Chemother* doi: 10.1128/AAC.00686-13 AAC.00686-13 (2014).
13. Andrews, K. T., Klatt, N., Adams, Y., Mischnick, P. & Schwartz-Albiez, R. Inhibition of chondroitin-4-sulfate-specific adhesion of *Plasmodium falciparum*-infected erythrocytes by sulfated polysaccharides. *Infect. Immun.* **73**, 4288–4294 (2005).
14. Schwartz-Albiez, R. *et al.* Regioselectively modified sulfated cellulose as prospective drug for treatment of malaria tropica. *Glycoconj J* **24**, 57–65 (2007).
15. Vogt, A. M. *et al.* Release of sequestered malaria parasites upon injection of a glycosaminoglycan. *PLoS Pathog* **2**, e100. doi:10.1371/journal.ppat.0020100 (2006).
16. Zhang, Y. *et al.* Proteomic analysis of *Plasmodium falciparum* schizonts reveals heaparin-binding merozoite proteins. *J. Proteome Res.* **12**, 2185–93 (2013).
17. Kobayashi, K. *et al.* Analyses of interactions between heparin and the apical surface proteins of *Plsamodium falciparum. Sci. Rep.* **3**, 3178 (2013).
18. Boyle, M. J., Richards, J. S., Gilson, P. R., Chai, W. & Beeson, J. G. Interactions with heparin-like molecules during erythrocyte invasion by *Plasmodium falciparum* merozoites. *Blood* **115**, 4559–4568 (2010).
19. Kobayashi, K. *et al. Plasmodium falciparum* BAEBL binds to heparan sulfate proteoglycans on the human erythrocyte surface. *J. Biol. Chem.* **285**, 1716–1725 (2010).
20. Wilson, D. W., Langer, C., Goodman, C. D., McFadden, G. I. & Beeson, J. G. Defining the timing of action of antimalarial drugs against *Plasmodium falciparum. Antimicrob. Agents Ch.* **57**, 1455–1467 (2013).
21. Lobo, C. A., Rodriguez, M., Reid, M. & Lustigman, S. Glycophorin C is the receptor for the *Plasmodium falciparum* erythrocyte binding ligand PfEBP-2 (baebl). *Blood* **101**, 4628–4631 (2003).
22. WHO. *Guidelines for the Treatment of Malaria - 2nd edition* (WHO Press, Geneva, 2010).
23. Adams, Y., Smith, S. L., Schwartz-Albiez, R. & Andrews, K. T. Carrageenans inhibit the *in vitro* growth of *Plasmodium falciparum* and cytoadhesion to CD36. *Parasitol. Res.* **97**, 290–294 (2005).
24. James, M. A. & Alger, N. E. *Plasmodium berghei*:effect of carrageenan on the course of infection in the A/J mouse. *Int. J. Parasitol.* **11**, 217–220 (1981).
25. Huber, J. D. *et al.* Blood-brain barrier tight junctions are altered during a 72-h exposure to λ-carrageenan-induced inflammatory pain. *Am. J. Physiol. Heart Circ. Physiol.* **283**, H1531–H1537 (2002).
26. Yuan, H. *et al.* Preparation and *in vitro* antioxidant activity of κ-carrageenan oligosaccharides and their oversulfated, acetylated, and phosphorylated derivatives. *Carbohydr. Res.* **340**, 685–692 (2005).
27. Yuan, H., Song, J., Li, X., Li, N. & Dai, J. Immunomodulation and antitumor activity of κ-carrageenan oligosaccharides. *Cancer Lett.* **243**, 228–234 (2006).
28. Yuan, H., Song, J., Li, X., Li, N. & Liu, S. Enhanced immunostimulatory and antitumor activity of diferent derivatives of κ-carrageenan oligosaccharides from *Kappaphycus striatum. J. Appl. Phycol.* **23**, 59–65 (2011).
29. Wang, F. F. *et al.* Antibacterial activities of kappa-carrageenan oligosaccharides (abstract). *Mechanical Engineering and Materials Science* **108**, 194–199 (2011).
30. Wang, W. *et al. In vitro* inhibitory effect of carrageenan oligosaccharide on influenza A H1N1 virus. *Antiviral Res.* **92**, 237–246 (2011).
31. Tang, F., Chen, F. & Li, F. Preparation and potential *in vivo* anti-influenza virus activity of low molecular-weight κ-carrageenans and their derivatives. *Journal of Appl. Polymer Sci.* **127**, 2110–2115 (2013).
32. Vlieghe, P. *et al.* Synthesis of new covalently bound κ-carrageenan-AZT conjugates with improved anti-HIV activities. *J. Med. Chem.* **45**, 1275–1283 (2002).
33. Ogaji, I. J., Nep, E. I. & Audu-Peter, J. D. Advances in natural polymers as pharmaceutical excipients. *Pharmaceutica Analytica Acta* **3**, 146 (2012).
34. Rinaudo, M. & Milas, M. *Novel Macromolecules in Food Systems – Developments in Food Science 41* (Elsevier Science B.V., Amsterdam:2000).
35. Shah, J. N., Jani, G. K. & Parikh, J. R. Gellan gum and its applications - a review. *Pharmaceutical Information, Articles and Blogs* **5**, http://www.pharmainfo.net/reviews/gellan-gum-and-its-application---review (2007). Accessed June 10, 2013.
36. Goncalves, V. M. F. *et al.* Structural analysis of gellans produced by *Sphingomonas elodea* strains by electrospray tandem mass spectrometry. *Carbohydr. Polym.* **77**, 10–19 (2009).
37. Lee, M. W., Tasi, H. F., Wen, S. M. & Huang, C. H. Photocrosslinkable gellan gum film as an anti-adhesion barrier. *Carbohydr Polym* **90**, 1132–8 (2012).
38. Chang, S. J. *et al.* Gellan gum films for effective gided bone regeneration. *J Med Biol Eng* **30**, 99–103 (2010).
39. Kim, M. Y., Lee, C. M., Kim, J. N., Cho, K. O. & Lee, K. Y. Prevention of post-surgical peritoneal adhesion in rats using curdlan and gellan gum hydrogels. *Macromol Res* doi: 10.1007/s13233-012-0184-1 (2012).
40. Silva-Correira, J. *et al.* Gellan gum-based hydrogels for intervertebral disc tissue-engineering applications. *J Tissue Eng Regen Med* **5**, e97–107 (2011).
41. Oliveira, J. T. *et al.* Gellan gum injectable hydrogels for cartilage tissue engineering applications: *in vitro* studies and preliminary *in vivo* evaluation. (abstract) *Tissue Eng Part A* **16**, 343–53 (2010).
42. Miyamoto, K. *et al.* Preparation of gellan sulfate as an artificial ligand for removal of extra domain A containing fibronectin. *Int. J. of Biol. Macromol.* **28**, 381–385 (2001).
43. Miyamoto, K. *et al.* Gellan sulfate selectively suppresses the activation of hemocoagulation factors XI and XII. *Mater. Sci. Eng. C* **30**, 364–368 (2010).
44. Jay, A. J. *et al.* Analysis of structure and function of gellans with different substitution patterns. *Carbohydr. Polym.* **35**, 179–188 (1998).
45. van de Velde, F. *et al.* H-1 and c-13 high resolution nmr spectroscopy of carrageenans: Application in research and industry. *Trends Food Sci. Tech.* **13**, 73-(2002).
46. van de Velde, F., Pereira, L. & Rollema, H. S. The revised nmr chemical shift data of carrageenans. *Carbohydr. Res.* **339**, 2309–2313 (2004).
47. de Araujo, C. A. *et al.* Selective sulfation of carrageenans and the influence of sulfate regiochemistry on anticoagulant properties. *Carbohydr. Polym.* **91**, 483–491 (2013).
48. Thahn, T. T. T., Yasunaga, H., Takano, R., Urakawa, H. & Kajiwara, K. Molecular characteristics and gelling properties of carrageenan family - 2. Tri-sulfated and tetra-sulfated carrageenans. *Polym. Bull.* **47**, 305–312 (2001).
49. Shih, S., Wang, Z., Guo, S. & Li, L. Anticoagulant activity of cellulose sulfates with different intrinsic viscosities. *Asian J. Pharmaceut. Sci.* **2**, 38–43 (2007).
50. Chen, J. H., Lim, J. D., Sohn, E. H., Cho, Y. S. & Han, E. T. Growth-inhibitory effect of a fucoidan from brown seaweed *Undaria pinnatifida* on *Plasmodium* parasites. *Parasitol. Res.* **104**, 245–250 (2009).
51. Ono, L. *et al. In vitro* and *in vivo* antiviral properties of sulfated galactomannans against yellow fever virus (BeH111 strain) and dengue 1 virus (Hawaii strain). *Antiviral Res.* **60**, 201–208 (2003).
52. Muschin, T., Kanamoto, T., Nakashima, H. & Yoshida, T. Synthesis and potent biological activities of sulfated galactomannans. *Poster presentation: The 9th SPSJ International Polymer Conference* (IPC2012) (2012).
53. Bo, S., Muschin, T., Kanamoto, T., Nakashima, H. & Yoshida, T. Sulfation and biological activities of konjac glucomannan. *Carbohydr. Polym.* **94**, 899–903 (2013).
54. Rochas, C., Lahaye, M. & Yaphe, W. Sulfate content of carrageenan and agar determined by infrared spectroscopy. *Botanica Marina* **29**, 335–340 (1986).
55. Melo, M. R. S., Feitosa, J. P. A., Freitas, A. L. P. & dePaula, R. C. M. Isolation and characterization of soluble sulfated polysaccharide from Gracilaria cornea. *Carbohydr. Polym.* **49**, 491–498 (2002).
56. Radfar, A. *et al.* Synchronous culture of *Plasmodium falciparum* at high parasitemia levels. *Nat. Protoc.* **4**, 1899–1915 (2009).
57. Persson, K. E. M., Lee, C. T., Marsh, K. & Beeson, J. G. Development and optimization of high-throughput method to measure *Plasmodium falciparum*-specific growth inhibitory antibodies. *J. Clin. Microbiol.* **44**, 1665–1673 (2006).
58. Bates, A. H., Mu, J., Jiang, H., Fairhurst, R. M. & Su, X. Use of magnetically purified *Plasmodium falciparum* parasites *improves the* accuracy of erythrocyte invasion assays. *Exp. Parasitol.* **126**, 278–280. (2010).

59. Spadafora, C., Gerena, L. & Kopydlowski, K. M. Comparison of the in vitro invasive capabilities of *Plasmodium falciparum* schizonts isolated by Percoll gradient or using magnetic beads separation. *Malar. J.* **10**, (2011).
60. Edmondson, J. M., Armstrong, L. S. & Martinez, A. O. A rapid and simple MTT-based spectrophotometric assay for determining drug sensitivity in monolayer cultures. *J. Tissue Cult. Meth.* **11**, 15–17 (1988).

Acknowledgments

This study was supported by Grants-in-Aids for Young Scientists, and Scientific Research on Innovative Areas (3308) from the Ministry of Education, Culture, Science, Sports, and Technology (MEXT) and for Research on global health issues from the Ministry of Health, Labour and Welfare of Japan, the Bio-oriented Technology Research Advancement Institution (BRAIN), The Naito Foundation, and the Program to Disseminate Tenure Tracking System from the Japan Science and Technology Agency (JST).
We would also like to thank Dr. Mizuki Tomihari and Dr. Kazuro Miyahara of the Veterinary Medical Center of the Obihiro University of Agriculture and Veterinary Medicine for providing resources and assistance in the conduct of the APTT anticoagulation assays.

Author contributions

F.C.R., K.K. and K.K. designed the experiments. F.C.R. performed the malaria and biological experiments and wrote the main manuscript. A.Ishiwa., Y.E.R. and N.G.V.F. prepared, analyzed and co-wrote the methods and discussion on the synthetic polysaccharides. T.S., H.T., T.I., F.M., H.G., A.I., T.H. and T.I. contributed to the data analysis and discussion. K.Kato edited the manuscript and supervised the study.

Additional information

Supplementary information accompanies this paper at http://www.nature.com/scientificreports

Competing financial interests: The authors declare no competing financial interests.

How to cite this article: Recuenco, F.C. *et al.* Gellan sulfate inhibits *Plasmodium falciparum* growth and invasion of red blood cells *in vitro*. *Sci. Rep.* 4, 4723; DOI:10.1038/srep04723 (2014).

SCIENTIFIC REPORTS

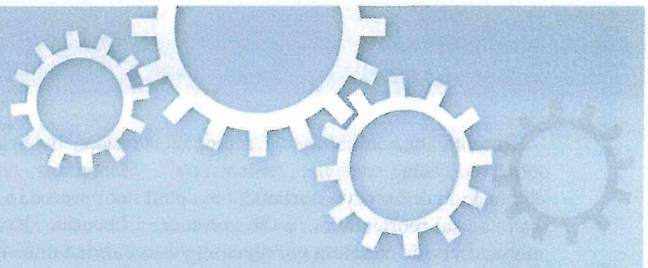

OPEN

SUBJECT AREAS:
PARASITE HOST RESPONSE
PATHOGENS
PARASITE BIOLOGY
CLINICAL MICROBIOLOGY

Received
9 May 2013

Accepted
23 October 2013

Published
11 November 2013

Correspondence and requests for materials should be addressed to K.K. (kkato@obihiro.ac.jp)

Analyses of Interactions Between Heparin and the Apical Surface Proteins of *Plasmodium falciparum*

Kyousuke Kobayashi[1,2,3], Ryo Takano[4], Hitoshi Takemae[1,4], Tatsuki Sugi[1,4], Akiko Ishiwa[1,4], Haiyan Gong[1], Frances C. Recuenco[1,4], Tatsuya Iwanaga[1], Taisuke Horimoto[1], Hiroomi Akashi[1] & Kentaro Kato[1,4]

[1]Department of Veterinary Microbiology, Graduate School of Agricultural and Life Sciences, the University of Tokyo, [2]Division of Stem Cell Processing, Center for Stem Cell Biology and Regenerative Medicine, Institute of Medical Science, the University of Tokyo, [3]Division of Host-Parasite Interaction, Department of Microbiology and Immunology, Institute of Medical Science, the University of Tokyo, [4]National Research Center for Protozoan Disease, Obihiro University of Agriculture and Veterinary Medicine.

Heparin, a sulfated glycoconjugate, reportedly inhibits the blood-stage growth of the malaria parasite *Plasmodium falciparum*. Elucidation of the inhibitory mechanism is valuable for developing novel invasion-blocking treatments based on heparin. Merozoite surface protein 1 has been reported as a candidate target of heparin; however, to better understand the molecular mechanisms involved, we characterized the molecules that bind to heparin during merozoite invasion. Here, we show that heparin binds only at the apical tip of the merozoite surface and that multiple heparin-binding proteins localize preferentially in the apical organelles. To identify heparin-binding proteins, parasite proteins were fractionated by means of heparin affinity chromatography and subjected to immunoblot analysis with ligand-specific antibodies. All tested members of the Duffy and reticulocyte binding-like families bound to heparin with diverse affinities. These findings suggest that heparin masks the apical surface of merozoites and blocks interaction with the erythrocyte membrane after initial attachment.

Malaria is a major infectious disease worldwide; approximately 219 million people are infected with malaria annually, more than 660,000 of whom die (WHO report, 2012)[1]. This disease is caused by the infection of human erythrocytes with a protozoan parasite of the genus *Plasmodium*. Four human-specific *Plasmodium* species are currently known, including *P. falciparum*, *P. vivax*, *P. malariae*, and *P. ovale*. Among these, *P. falciparum* causes the most virulent form of human malaria.

This parasite has two hosts: female mosquitoes of the genus *Anopheles* and humans. Sexual reproduction occurs in the mosquitoes, and intra-erythrocytic proliferation takes place in the human bloodstream via repeated cycles of erythrocyte invasion, cell division, and cell rupture. The process by which parasitic merozoites invade erythrocytes involves the following steps: attachment, apical reorientation, junction formation, and formation of a protective parasitophorous vacuole[2,3].

Each invasion step is mediated by various proteins. In the initial attachment, merozoite surface proteins (MSPs) are thought to play an important role[4]. Apical membrane antigen-1 (AMA1) is believed to mediate active invasion by associating with rhoptry neck proteins (RONs)[5,6]. A number of factors are thought to mediate junction formation between merozoites and erythrocytes through sialic acid–dependent and –independent pathways; these factors include the Duffy binding-like (DBL) family that contains erythrocyte-binding antigen-175 (EBA-175), BAEBL (also known as EBA-140), JESEBL (also known as EBA-181), and EBL-1; and the reticulocyte binding-like (RBL) family, which contains *P. falciparum* reticulocyte-binding homolog 1 (PfRH1), PfRH2a, PfRH2b, PfRH4, and PfRH5[7]. These molecules recognize specific receptors on the erythrocyte surface, some of which have been identified, for example glycophorin A is a receptor for EBA-175, glycophorin B for EBL-1, glycophorin C for BAEBL, complement receptor 1 for PfRH4, and basigin for PfRH5[7]. The function of the DBL and RBL proteins are redundant because knockout strains of all of the *dbl* and *rbl* genes except for PfRH5 have been generated and show insignificant loss of invasion efficiency[7].

Because the clinical manifestations of malaria are caused by asexual blood-stage parasites, a study of *P. falciparum* in this stage is important for developing effective treatments for malaria. In fact, almost all antimalarial drugs inhibit parasite growth through a blood stage–specific mechanism. However, parasites resistant to these drugs have emerged[8,9] highlighting the need for novel drug targets.

Recently, the inhibition of merozoite invasion by heparin was observed using real-time microscopy[10]. Merozoites reportedly attached to erythrocytes normally but could not proceed to the next step, apical reorientation, in the presence of heparin. Heparin is a polysaccharide consisting of repeating disaccharide units of an uronic acid molecule and a glucosamine molecule; it has abundant sulfate groups that confer its anionic charge. Several studies have reported the importance of these sulfate groups for the inhibitory activity of heparin[10,11] and various sulfated polysaccharides, such as curdlan sulfate, dextran sulfate, pentosan sulfate, and fucoidan, λ- and ι-carrageenans, as well as heparin and heparan sulfate (HS), inhibit the growth of blood-stage parasites *in vitro*[11–15], although some sulfated polysaccharides, such as κ-carrageenan and chondroitin sulfates A (CSA) and C show no apparent inhibition[11,14,15]. Some sulfated polysaccharides including dextran sulfate[16] and fucoidan[17] have shown *in vivo* inhibitory activity in the blood-stage growth of *P. berghei*. In addition, artificially sulfated compounds, such as (poly)-vinylsulfonate[18] and sulfated cyclodextrin[19], also reportedly inhibited growth *in vitro* and *in vivo*. These studies collective suggest that sulfated compounds have promise as novel antimalarial agents.

Although the inhibitory mechanism remains uncertain, our previous study showed that the addition of soluble heparin and HS inhibited the binding of BAEBL to erythrocytes by competitively inhibiting the binding to HS on the erythrocyte surface[20,21]. However, this finding was not sufficient to explain the nearly complete invasion inhibition by heparin because BAEBL is not an essential ligand for the invasion[22]. Erythrocyte binding of some parasite ligands, including full-length MSP1, the C-terminal 42-kDa fragment of MSP1 (MSP1-42), and PfRH5 is disrupted by heparin[10,11,23], raising the possibility that heparin-induced inhibition of the binding of multiple ligands results in invasion inhibition.

In this study, to better understand the mechanisms of invasion inhibition by sulfated polysaccharides, we examined the binding of heparin (as a model of a sulfated polysaccharide) to merozoite proteins or to the merozoite surface. Many molecules derived from parasite cultures, including erythrocyte-binding proteins, were found to interact with heparin. Further characterization demonstrated that the heparin-binding proteins are primarily localized in the apical organelles and are secreted to the apical tip. We found that proteins in the DBL and RBL families bound to heparin, and that some of them bound with high affinity. These results suggest that heparin-induced disruption of the interaction between the apical surface of merozoites and the erythrocyte surface contributes to invasion inhibition. This finding provides useful information for the development of novel antimalarial drugs and for understanding the role of HS on the erythrocyte surface during merozoite invasion.

Results

Heparin binding to the erythrocyte surface does not cause invasion inhibition of merozoite. Several previous studies have suggested that heparin or other anion saccharides inhibit the invasion of *P. falciparum* merozoites[10,11,13,14,18,19,21,24], and some reports have suggested that the molecular targets of heparin are the merozoite proteins[10,21,23]. However, no report has excluded erythrocyte proteins as candidate targets. To investigate whether heparin has inhibitory effects on the susceptibility of erythrocytes to merozoites, we assessed merozoite invasion of erythrocytes that were preincubated with heparin (Fig. 1). When the erythrocytes were not washed, merozoites were unable to invade due to the presence of heparin. However, after washing, the susceptibility of the erythrocytes to merozoite invasion was restored to the same levels as in the control erythrocytes in the absence of heparin. These results suggest that heparin decreases the infectivity of merozoites, but not the susceptibility to erythrocytes.

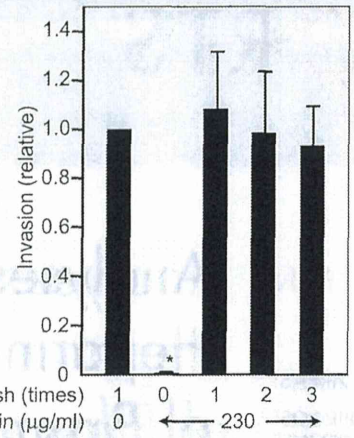

Figure 1 | The binding of heparin to the erythrocyte surface does not inhibit merozoite invasion. Three microliters of packed erythrocytes were mixed with CM in the absence or presence of 230 μg/mL heparin and incubated at 37°C overnight. The erythrocytes were washed 0–3 times before being used for the invasion assays. The invasion rates were calculated by dividing the parasitemia of the test cultures by that of the cultures that lacked heparin. The results are shown as the means of three independent experiments, and the error bars represent standard errors. The asterisk (*) indicates significant differences ($p < 0.05$) as determined by *t*-tests.

Heparin interacts with the merozoite surface. To investigate whether heparin interacts with the merozoite surface, we examined the binding between intact merozoites and heparin-agarose beads (Fig. 2). Several GFP- expressing merozoites stained with DAPI were observed on the surface of heparin-agarose beads (Fig. 2A). In the binding assay, the addition of soluble heparin decreased the punctate nuclear-staining pattern of the merozoites on the beads surface but not the diffuse pattern of background signals (Fig. 2B middle panel). On the other hand, the addition of soluble CSA, which has no or little inhibitory effect on merozoite invasion, caused no apparent decrease in merozoite binding to the bead surface (Fig. 2B right panel). This result demonstrates that the merozoite surface attaches to the heparin-agarose beads specifically and suggests that some heparin-binding proteins are expressed on the merozoite surface.

To prove that biotinylated heparin has the same binding properties as heparin, we demonstrated that biotinylated heparin correctly recognizes the surface of infected erythrocytes, as shown previously[25] (Fig. 3A). In addition, biotinylated heparin inhibited merozoite invasion at the same level as did unlabeled heparin (Fig. 3B). These results demonstrate that biotinylation has no effect on the nature of heparin. Isolated merozoites were incubated with biotinylated heparin and analyzed by means of flow cytometry (Fig. 3C). This assay detected the binding of biotinylated heparin to the merozoite surface. In addition, this binding was competitively inhibited by unlabeled heparin, indicating that biotinylated and unlabeled heparin recognize identical targets.

To detect the localization of heparin-binding proteins on the surface of merozoites, the merozoites treated with biotinylated heparin were observed by using confocal laser scanning microscopy (Fig. 3D). Heparin showed a similar localization pattern to that of EBA-175, demonstrating that heparin binds predominantly to the tip of the apical end.

Organelles containing abundant heparin-binding proteins were detected by observing biotinylated heparin bound to fixed and permeabilized merozoites on a glass slide (Fig. 3E). Compared with the localization of EBA-175 (microneme), MSP1-19 (surface), and the nucleus, heparin-binding proteins were found to be more abundant in the apical organelles, such as the micronemes and/or rhoptries.

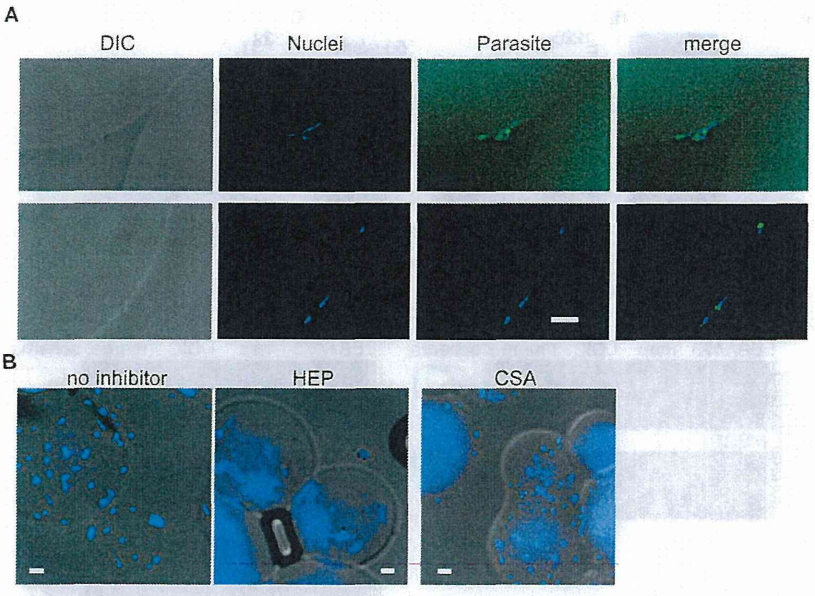

Figure 2 | Merozoites bind to heparin-agarose beads. (A) Heparin-agarose beads were incubated with a GFP-expressing parasite culture in the late schizont stage until the number of egressing merozoites increased. The beads separated from erythrocytes were washed, fixed, and stained with DAPI (nuclei). In this panel, differential interference contrast (DIC) images, fluorescent signals of the parasite nuclei and GFP, and the merged signals are shown. (B) During incubation of the beads with parasite cultures, 10 mg/mL soluble heparin (HEP), CSA, or PBS (no inhibitor) was added. After being collected, washed, and fixed, the beads were stained with TO-PRO-3. In panels A and B, the white bars represent 5 μm.

Many parasite proteins interact with heparin. To examine whether various proteins could bind to heparin, we incubated ^{35}S-labeled parasite proteins with a series of coated agarose beads and subjected them to autoradiography (Fig. 4A). Numerous parasite proteins bound to heparin-agarose beads, whereas no proteins bound to glutathione-Sepharose, Ni-NTA–agarose, or protein G-Sepharose beads.

Next, we evaluated the erythrocyte-binding potential of the parasite proteins adsorbed to the heparin-agarose beads. After adsorption to the beads, unbound proteins were subjected to an erythrocyte-binding assay (Fig. 4B). The number of erythrocyte-binding proteins was drastically decreased by adsorption to heparin-agarose but not to glutathione-Sepharose beads. These results demonstrate that erythrocyte-binding proteins also bind to heparin.

Heparin-binding proteins can be separated from the schizont lysate by use of affinity chromatography with a heparin column. Taken together, the above findings suggest that heparin interacts with many erythrocyte-binding proteins secreted from the apical organelles to the apical surface. These characteristics closely resemble those of ligand molecules that mediate junction formation. Heparin has been reported to disrupt the erythrocyte binding of several ligand molecules involved in junction formation, including BAEBL[21] and PfRH5[23]. We, therefore, hypothesized that heparin might inhibit the binding of additional proteins involved in junction formation.

To isolate proteins that interact with heparin, we used affinity chromatography with a HiTrap heparin HP column (Fig. 5A). In this method, proteins weakly bound to heparin are eluted in buffer containing a lower concentration of NaCl. The collected fractions are then analyzed by SDS-PAGE, followed by silver staining (Fig. 5B). In the E2–9 fractions, clear bands were detected, and the band patterns observed in each lane were reproducible.

The flow through (FT) and E3–9 fractions were analyzed by immunoblot analysis using specific antibodies against well-known ligands that mediate merozoite invasion. A full-length form of AMA1 (AMA1–83) was the most abundant in the FT but was detectable in E3–9 fractions, consistent with a previous report suggesting non-specific binding between heparin and AMA1[10]. A 66-kDa processed form of AMA1 (AMA1–66), however, did not bind to heparin and was detected only in the FT fraction, whereas the shorter forms of AMA1 (AMA1–52, AMA1–48, and AMA1–44) bound to heparin and were eluted in the E3–5 fractions. PfRON2 was also eluted in the E3–5 fractions. Although these two proteins and other RON members reportedly form a complex during invasion, it is not certain whether they bind to heparin as a complex.

The full-length and all processed forms of MSP1 containing the C-terminal region corresponding to MSP1–42 bound to heparin and were eluted in the E3–5 fractions. Therefore, the binding was relatively weak.

Among the DBL and RBL family members, BAEBL and PfRH1 showed the highest affinity for heparin (eluted in E9), whereas EBA-175, JESEBL, and PfRH4 showed lower affinity (eluted in E3–5), as did MSP1. PfRH2 and PfRH5 (eluted in E6 and E7) showed greater affinity than did EBA-175, JESEBL, and PfRH4. These results indicate that all tested members of the DBL and RBL families bind heparin with different affinities. The ligands with relatively high affinity (BAEBL, PfRH1, PfRH2, and PfRH5) are associated with junction formation and localize to micronemes or rhoptries, consistent with the localization of the heparin-binding proteins shown in Figure 3.

Approximately 30% of the total parasite proteins, however, were detected in the bound and eluted fractions. Since it is unlikely that heparin-binding proteins constitute such a significant fraction of the total parasite proteins, we speculated that some parts of the eluted proteins bound to the column with relatively low specificity. To confirm the specificity, parasite proteins binding to the heparin affinity column were competitively eluted with increasing concentrations of soluble heparin. From 500 μg/mL to 10 mg/mL, eluted proteins were detected by silver staining (Fig. 6A), suggesting that these proteins specifically recognized heparin. However, approximately 42% of the total proteins bound to the column were not eluted by up to 10 mg/mL heparin but were eluted by 2 M NaCl (Fig. 6B). These proteins theoretically contained two possible types: proteins that bound to the column nonspecifically and/or proteins that bound to heparin with too high an affinity to be eluted by 10 mg/mL heparin.

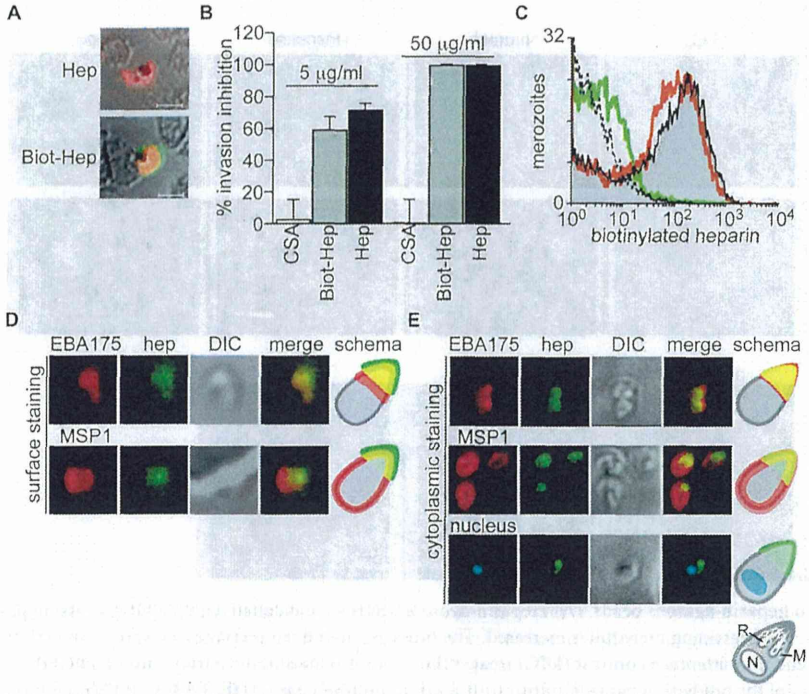

Figure 3 | Heparin-binding proteins localize predominantly at the apical ends of merozoites. (A) The binding specificity of biotinylated heparin was verified. A parasite culture in the late schizont stage was smeared onto glass slides, fixed with methanol, and treated with a rabbit anti-EBA-175 antibody (red) and either unlabeled heparin (Hep) or biotinylated heparin (Biot-Hep; green). Signals were detected by using streptavidin–Alexa Fluor 488 and Alexa Fluor 633 secondary antibodies. The white bars represent 5 μm. (B) Invasion inhibitory activity of biotinylated heparin. Invasion inhibition assays were performed in the presence of 5 or 50 μg/mL CSA, biotinylated heparin (Biot-Hep), or unlabeled heparin (Hep). The percentages of invasion inhibition were calculated by dividing the parasitemia of the test cultures by that of the control cultures, multiplying the result by 100, and then subtracting the result from 100. The results are shown as the means of three independent experiments; the error bars represent standard errors. (C) Binding between heparin and merozoite surfaces. Parasite cultures at the late schizont stage were cultured with 50 μg/mL biotinylated heparin in the absence (grey) or presence of 1 mg/mL heparin (green line) or CSA (red line) for 1 h. Free merozoites were isolated from the culture supernatant, stained with fluorescent streptavidin, and analyzed by flow cytometry. The dashed line shows untreated merozoites. (D) The heparin binding site on the merozoite surface. Biotinylated heparin was incubated with a parasite culture at the late schizont stage. When the number of egressing merozoites increased, the culture was fixed and stained with an antibody against EBA-175 (apical end) or MSP1–19 (surface). The biotinylated heparin and the antibody on the parasite surface were visualized by using fluorescent-labeled streptavidin or secondary antibodies. (E) Localization of heparin-binding proteins in merozoites. The localization of heparin-binding proteins was compared with EBA-175 (microneme and apical end), MSP1–19 (surface), or nuclei by immunofluorescent staining using biotinylated heparin, specific antibodies, and TO-PRO-3. (D), (E) The fluorescent signals of the marker proteins and heparin (hep), DIC images, merged fluorescent signals, and a schematic for their localization are shown. M, micronemes; R, rhoptries; N, nuclei.

The FT and fractions eluted with 500–10,000 μg/mL heparin and with 2 M NaCl were analyzed by immunoblotting using specific antibodies against MSP1 and the DBL and RBL proteins (Fig. 6C). All tested proteins were eluted by soluble heparin, suggesting that these proteins bind to heparin specifically. Two of these proteins, BAEBL and PfRH5, were eluted incompletely by 10 mg/mL heparin, suggesting that they have an extremely high affinity for heparin. The affinity determined by heparin elution should more faithfully represent the affinity to heparin than that determined by NaCl elution.

Heparin disaccharides (HDS) 1-S and CSA were used as control competitors, because inhibition of invasion by these compounds is much less efficiently than that by heparin[10,11,14]. In particular, because HDS 1-S were generated by digestion of heparin with heparinases and contain three major sulfate groups (*N*-, 2-*O*-, and 6-*O*-sulfate groups), the same concentration of heparin and HDS 1-S carry almost the same amount of negative charge. If only negative charge is important for binding to parasite proteins, HDS and/or CSA should also elute parasite proteins bound to the heparin-affinity column. However, few protein bands were detected in the fractions eluted by 1000–10000 μg/mL HDS, and no apparent bands were detected in the fractions eluted by CSA (Fig. 6A). A smaller proportion of proteins relative to the total proteins bound to the column were eluted by HDS (*ca.* 30%) and CSA (*ca.* 25%) compared with heparin (*ca.* 58%) (Fig. 6B). The proteins eluted by HDS were assumed to bind to heparin only by electrostatic interaction or by specific recognition of a disaccharide unit. For these proteins, no parasite proteins associated with merozoite invasion were detected by immunoblotting (Fig. 6D).

Clone-specific disruption of the AMA1/RONs complex by heparin contributes little to the inhibition of invasion. It was recently revealed that the AMA1/RONs complex has a critical role in the merozoite invasion of *P. falciparum*[5,6,26]. Because we observed a relatively weak interaction between heparin and the complex components (AMA1 and RON2), we investigated the possibility that heparin inhibits AMA1/RONs complex formation.

As shown previously[27], the bands corresponding to RON2, RON4, and RON5 coimmunoprecipitated with AMA1 (Fig. 7A). These bands from the 3D7 clone disappeared with the addition of the R1 peptide, whereas those from the HB3 clone did not. This R1 peptide reportedly binds to AMA1 and inhibits complex formation and merozoite invasion in a clone-specific manner; R1 peptide is effective for the 3D7 clone but not for the HB3 clone[5,28]. We confirmed this

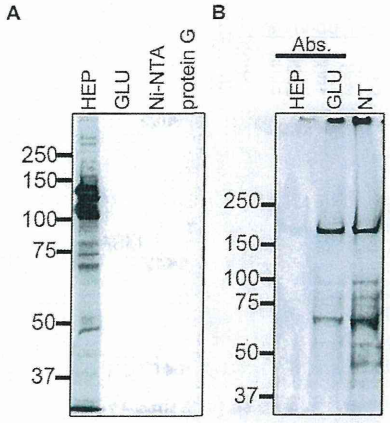

Figure 4 | Erythrocyte-binding proteins of parasites bind to heparin-agarose beads. (A) Pull-down assays of radiolabeled culture supernatants of *P. falciparum* using heparin-agarose (HEP), glutathione-Sepharose (GLU), Ni-NTA–agarose, or protein G-Sepharose beads. (B) Erythrocyte-binding assays of radiolabeled culture supernatants, which were pre-adsorbed to heparin-agarose (HEP) or glutathione-Sepharose (GLU) beads or were not pre-adsorbed (NT). Proteins that bound to the beads or erythrocytes were eluted and analyzed by means of autoradiography. The molecular masses (kDa) are indicated on the left.

specificity in our system and confirmed that the bands are RONs, consistent with previous reports.

Next, by using this assay, we examined whether heparin or CSA affects the complex formation (Fig. 7B). In the case of the HB3 clone, neither heparin nor CSA significantly decreased the coprecipitation of RON2 or RON4. Although RON5 of the HB3 clone appeared to be decreased by CSA (Fig. 7B), no such decrease occurred in any other experiments (data not shown). Densitometric analysis showed that formation of the complex between AMA1 and RONs was inhibited partially by the addition of either heparin or CSA (Fig. 7C), suggesting that, to induce the invasion inhibition, heparin targets molecular events other than those involving AMA1 and RONs. On the other hand, in the case of the 3D7 clone, AMA1/RONs complex formation was clearly inhibited by heparin but not by CSA. Densitometric analysis showed that the complex was partially disrupted by the addition of heparin but almost completely disrupted by the R1 peptide. These results demonstrate that heparin inhibits AMA1/RONs complex formation in a clone-specific manner.

If this heparin-induced complex disruption is a key factor for the invasion inhibition by heparin, heparin would be expected to cause no significant invasion inhibition of the HB3 clone. However, contrary to this expectation and without disruption of AMA1/RONs complex formation, heparin inhibited the invasion of the HB3 clone (Fig. 7D). Accordingly, disruption of this complex formation is not a true target of heparin.

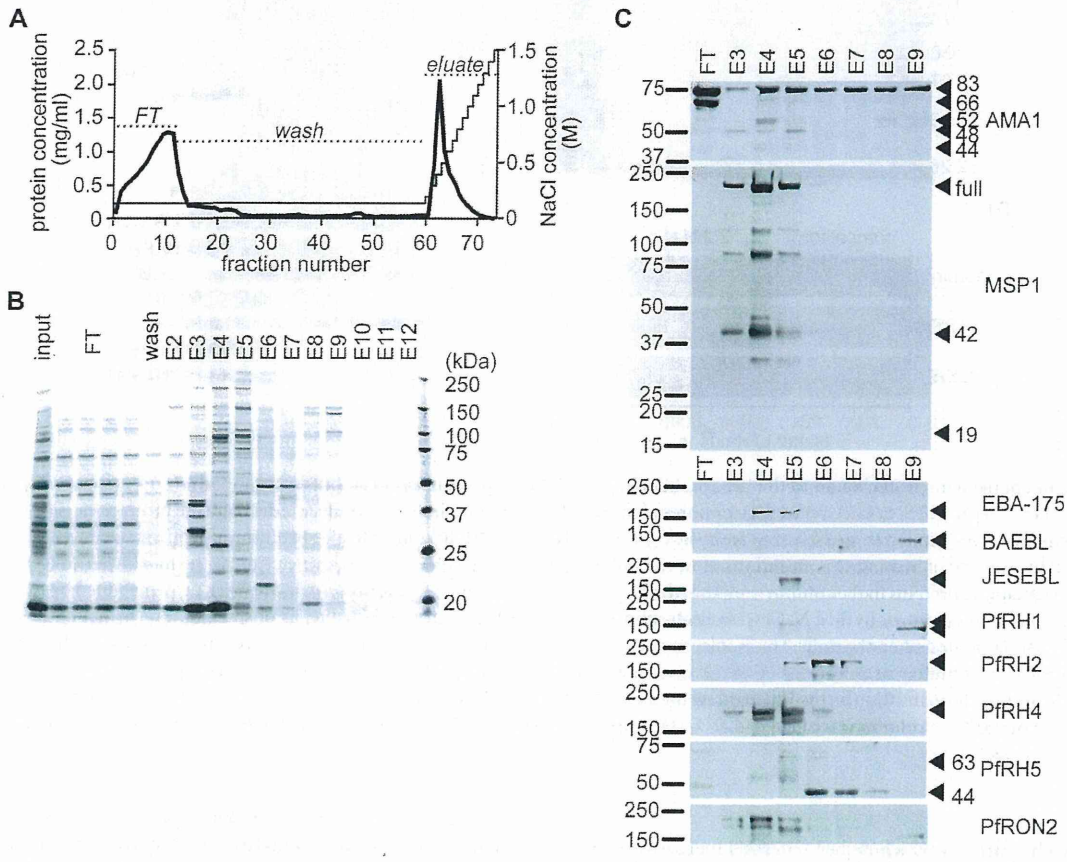

Figure 5 | Affinity chromatography of schizont proteins on a heparin column. (A) The elution profile of heparin-binding proteins of the *P. falciparum* HB3 clone. A schizont lysate was diluted with the binding buffer and separated by affinity chromatography on a heparin column. The proteins were washed and eluted from the column with a stepwise gradient of NaCl (0.2–1.5 M; thin line). Flow-through fractions of the lysate (FT), the wash buffer (wash), and the elution buffer (eluate) were collected (1.0 mL each) and subjected to protein quantification (thick line). (B) The eluate fractions containing proteins (E2–12) were analyzed by use of SDS-PAGE and silver staining. The molecular masses (kDa) are indicated on the right. (C) Eight fractions (FT and E3–9) were analyzed by immunoblotting. The arrowheads indicate specific bands. The molecular masses (kDa) are indicated on the left.

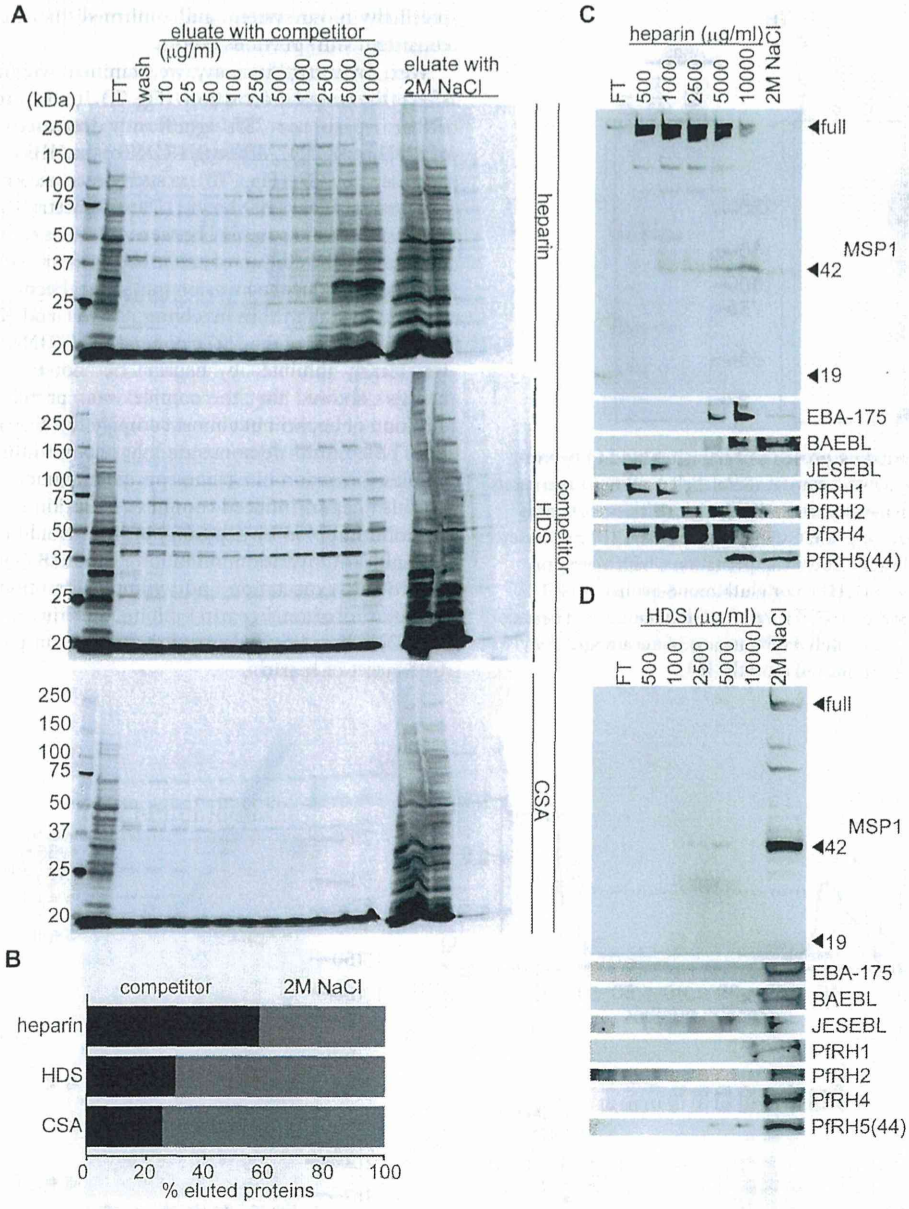

Figure 6 | Elution of parasite proteins bound to the heparin column by soluble heparin or other sulfated compounds. (A) Parasite proteins eluted by soluble competitors (heparin, HDS, or CSA) were electrophoresed on SDS-PAGE and subjected to silver staining. Parasite proteins capable of binding to the heparin column were separated from a schizont lysate by using a HiTrap Heparin HP column with a bed volume of 1 mL, washed with 10 mL of wash buffer, and eluted by 1 mL of increasing concentrations of the soluble competitors. After the competitive elution at the maximum concentration of 10 mg/mL, the remaining proteins in the column were eluted with 2 M NaCl. Flow-through fractions of the lysate (FT), proteins eluted by the wash buffer (wash), by the soluble competitors, or by 2 M NaCl were electrophoresed on SDS-PAGE and subjected to silver staining. The names of the competitors used for the elution are indicated on the right. The molecular masses (kDa) are indicated on the left. (B) The protein amount eluted by the competitors or NaCl was estimated by quantitative densitometry of the silver-stained gel using Image J software (ver. 1.45 s), because heparin in the eluted fractions interfered with the protein quantification by the Bradford method as used in Fig. 5. The ratios of eluted proteins (by either the competitors or 2 M NaCl) to total proteins bound to the column was calculated. (C), (D) An unbound fraction (FT) and bound/eluted fractions with heparin (C) or HDS (D) were analyzed by immunoblotting.

Discussion

To reveal the mechanisms by which heparin inhibits merozoite invasion, it is important to understand when the inhibition occurs and whether this inhibition results from heparin interaction with the host cells or with the parasites. Previous studies found that heparin had little to no effect on the intracellular development of schizont- or ring-stage parasites[10,11,24]. Instead, direct evidence using real-time microscopy suggested that heparin inhibits merozoite invasion[10]; however, it remained clear whether heparin targets merozoites or erythrocytes for invasion inhibition. This study showed that heparin has an insignificant effect on erythrocytes with regard to merozoite invasion. Therefore, future studies should focus on interactions between merozoites and heparin to reveal the inhibitory mechanisms of heparin.

We found that various parasite proteins bind to heparin, by using pull-down assays of ^{35}S-labeled parasite proteins and heparin affinity